THE ASTROPHYSICAL JOURNAL, 421:762–770, 1994 February 1


# THE TEMPORAL EVOLUTION OF THE 4–14 MICRON SPECTRUM OF V1974 CYGNI (NOVA CYGNI 1992)

R. D. GEHRZ
Department of Astronomy, School of Physics and Astronomy, 116 Church Street, SE, University of Minnesota, Minneapolis, MN 55455
gehrz@ast1.spa.umn.edu

CHARLES E. WOODWARD[1]
Wyoming Infrared Observatory, Department of Physics and Astronomy, University of Wyoming, Laramie, WY 82071-3905
chelsea@wapiti.uwyo.edu

M. A. GREENHOUSE
Laboratory for Astrophysics, MRC 321, National Air and Space Museum, Smithsonian Institution, Washington, DC 20560
matt@wright.nasm.edu

S. STARRFIELD
Department of Physics and Astronomy, Arizona State University, Tempe, AZ 85287
starrfie@hyrdo.la.asu.edu

D. H. WOODEN, F. C. WITTEBORN, S. A. SANDFORD, L. J. ALLAMANDOLA, AND J. D. BREGMAN
NASA/Ames Research Center, Space Science Division, Moffet Field, CA 94035
wooden@ssa1.arc.nasa.gov, witteborn@ssa1.arc.nasa.gov, sandford@ssa1.arc.nasa.gov
allamandola@ssa1.arc.nasa.gov, bregman@ssa1.arc.nasa.gov

AND

M. KLAPISCH
Artep Inc., Naval Research Laboratory, Code 4894, Washington, DC 20375
*Received 1993 June 17; accepted 1993 July 17*

## ABSTRACT

We present 4–14 $\mu$m spectra of the ONeMg nova V1974 Cygni (Nova Cygni 1992) obtained during 1992 May on the NASA Kuiper Airborne Observatory (KAO) and from the NASA 1.52 m infrared telescope at Mount Lemmon, Arizona in 1992 October/November with the HIFOGS mid-infrared spectrometer. The spectra at both epochs showed continuum emission from thermal bremstrahlung (free-free radiation) with emission lines from hydrogen and [Ne II], [Ar III], and [Ne VI]. During May, $\approx$80 days after outburst, the dominant emission lines in the mid-infrared spectra were a blend of three hydrogen lines (Pf$\alpha$, Hu$\beta$, H11–7) near 7.5 $\mu$m and [Ne II] at 12.8 $\mu$m. By October ($\approx$160 days later), the hydrogen emission had virtually disappeared, the [Ne II] 12.8 $\mu$m line had weakened considerably, and a pronounced [Ne VI] emission line had appeared at 7.6 $\mu$m. This behavior confirms that V1974 Cyg is similar to the prototypical slow ONeMg "neon nova," Nova QU Vulpeculae (1984 No. 2). The remarkable evolution of the spectrum suggests that the ionization conditions changed drastically between 1992 May and 1992 October. We find that the ejecta of V1974 Cyg were overabundant in neon with respect to silicon by a factor of $\approx$10 relative to the solar photosphere. We present new model calculations of infrared sodium forbidden line emission from [Na III] 7.319 $\mu$m, [Na IV] 9.039 $\mu$m, and [Na IV] 21.29 $\mu$m that can be compared with recent model predictions of sodium synthesis in ONeMg nova outbursts. We conclude that sodium abundances in ONeMg novae can be determined by observations of infrared coronal lines of sodium that are accessible to the *Infrared Space Observatory* (*ISO*) and instruments at the NASA IRTF.

*Subject headings:* infrared: stars — novae, cataclysmic variables — radiation mechanisms: nonthermal — stars: abundances — stars: individual (Nova Cygni 1992)

## 1. INTRODUCTION

Infrared spectroscopy of V1974 Cyg (Nova Cygni 1992) reported by Hayward et al. (1992) showed that the evolution of neon emission in the ejecta was similar to that observed in the archetype "slow" ONeMg Nova QU Vulpeculae 1984 No. 2 (hereafter QU Vul; Gehrz, Grasdalen, & Hackwell 1985). These novae are characterized in the infrared by strong [Ne II] 12.8 $\mu$m emission that peaks within a few months after outburst. Optical spectra of these novae show strong [Ne V] emission at wavelengths shortward of 3400 Å and ultraviolet spectra exhibit strong Mg II 2800 Å and both [Ne IV] 1602 Å and [Ne V] 1575 Å emission (Dopita et al. 1993; Saizar et al. 1992). Abundance analyses of the material ejected by these novae show that oxygen, neon, aluminum, and magnesium are enhanced over a solar mixture of elements which gives rise to the ONeMg classification.

A strong [Ne VI] line at 7.63 $\mu$m dominated the shell emission of QU Vul 581 days after the eruption (Greenhouse et al. 1988). This was the first time this line was ever observed in an astrophysical source. The [Ne VI] 7.63 $\mu$m emission line also was detected in V1974 Cyg on day 264 after outburst. Abundances derived from the ultraviolet and 12.8 $\mu$m neon emission lines showed that both QU Vul and V1974 Cyg are overabundant in neon with respect to the solar photosphere (Saizar et al. 1992; Hayward et al. 1992). It has been suggested that novae such as these result from thermonuclear runaways (TNRs) on the surfaces of ONeMg white dwarfs accreting

[1] NSF Young Investigator.

matter in binary systems (Starrfield, Sparks, & Truran 1986; Gehrz, Truran, & Williams 1991). Observations of several ONeMg novae show that strong neon emission lines and other infrared coronal lines (forbidden lines of ions with ionization potential $\chi \geq 100$ eV) mark a characteristic phase of their spectral evolution (Greenhouse et al. 1990).

One isotope of great importance to the study of this class of novae is $^{22}$Na, which has a half-life of 2.6 yr. Recent theoretical calculations of TNRs on massive white dwarfs suggest that a sufficient amount of $^{22}$Na is synthesized in an ONeMg nova outburst for its decay to be detected by the *Compton GRO* (Starrfield et al. 1992b). This prediction could be confirmed if one could obtain a sodium abundance in an ONeMg novae. Previous observational studies of the sodium abundance in novae relied on analysis of a nebular emission line at 2069 Å (Williams et al. 1985), but it has recently been demonstrated that this line identification is incorrect (Shore et al. 1994). However, there are mid-infrared sodium "coronal lines" that can provide an accurate determination of the abundance.

Here we present new 4–14 $\mu$m infrared spectra obtained with airborne and ground-based telescopes showing that the temporal evolution of the infrared neon emission lines in V1974 Cyg and QU Vul were similar. We derive for V1974 Cyg a coronal zone ionization temperature, a Ne/Si abundance ratio for the ejecta, and an upper limit to the sodium emission expected from model Na/Si predictions. We present new detailed balance calculations and line emissivities to facilitate the search for infrared sodium lines in other ONeMg novae. Finally, we present model line ratios among sodium and silicon infrared coronal lines that reveal the prospects for observing infrared sodium emission in ONeMg outbursts.

## 2. OBSERVATIONS

The 4–14 $\mu$m spectra of V1974 Cyg were obtained using the NASA/Ames Research Center *H*igh efficiency *I*nfrared *F*aint *O*bject *G*rating *S*pectrometer—HIFOGS (Witteborn et al. 1991) at four separate epochs between 1992 May and 1992 November. Observations on 1992 May 7.4 UT (day 79) and 1992 May 15.4 UT (day 87) were made from the Kuiper Airborne Observatory (KAO) operating at an altitude of $\approx$12.5 km. Additional observations obtained on 1992 October 17.1 UT (day 242) and 1992 November 8.1 UT (day 264) were conducted with HIFOGS mounted at the Cassegrain focus of the NASA 1.52 m infrared telescope at Mount Lemmon, AZ. These spectra are presented in Figures 1–5. We adopt 1992 February 19 UT (JD 2,448,671) as day 0 for V1974 Cyg.

The spectrometer entrance aperture was 1.5 mm, providing 20″ and 12″ diameter fields of view on the KAO and the NASA 1.52 m, respectively. On the KAO, the 4.7–9.2 $\mu$m spectrum was dispersed across 100 detector channels at two slightly different grating angles (displaced by 7.5 channels) to provide a Nyquist-sampled resolving power of 180 over most of the spectral range. A different grating was used at a single angle to sample the 7.2–14.3 $\mu$m range at about 0.1 $\mu$m intervals. Wavelengths were calibrated by taking comparison spectra of polystyrene in absorption each time the grating angle was changed. The spectra are compared over the entire spectral range with a laboratory polystyrene spectrum referenced directly to a HeNe laser line. The flux standard on the KAO observations was Arcturus ($\alpha$ Boo) which was observed on the same flight at slightly lower air mass (1.12 vs. 1.31) than the nova. The standard used at Mount Lemmon was Aldebaran ($\alpha$ Tau), where it was observed at several air masses bracketing those through which V1974 Cyg was observed. An interpolation procedure was used to determine a standard spectrum with matching air mass. The fluxes adopted for flux standards are based on those of Cohen et al. (1992). These reference spectra are described in detail and tabulated by Walker & Cohen (1992).

## 3. DISCUSSION

It is evident from Figures 1–5 that the spectra at both the 1992 May ($\approx$day 80) and 1992 October/November ($\approx$day 260) epochs showed continuum emission from thermal bremstrahlung (free-free radiation), in part inferred from the observed 1–10 $\mu$m broad-band colors (Gehrz, Lawrence, & Jones 1992; Woodward & Gehrz 1992), with superposed emission lines. We

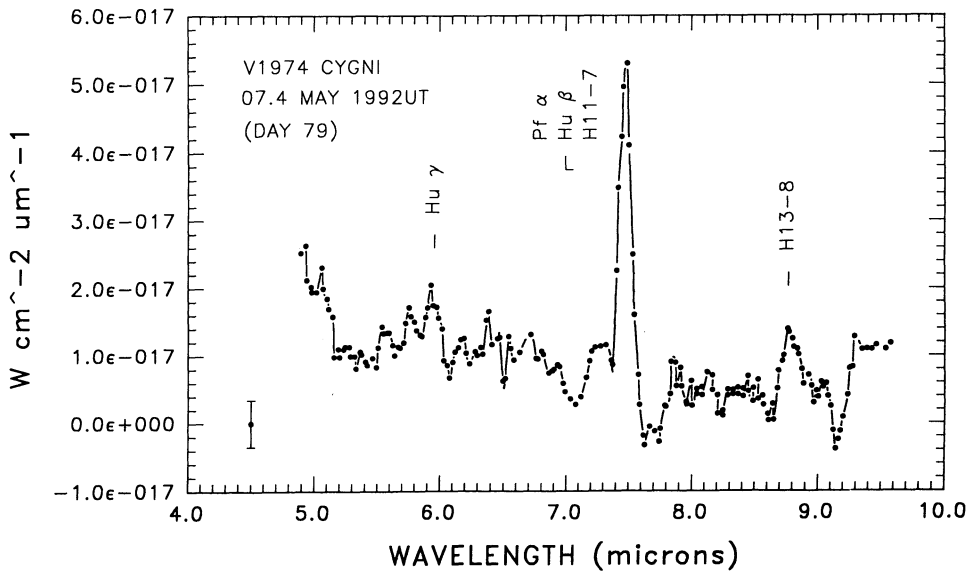


FIG. 1.—The 5–10 $\mu$m spectrum of V1974 Cyg obtained on 1992 May 7.4 UT (day 79) from the KAO. Prominent in the spectra are hydrogen recombination lines. A representative mean 1 $\sigma$ error bar is given in the lower left of the panel.

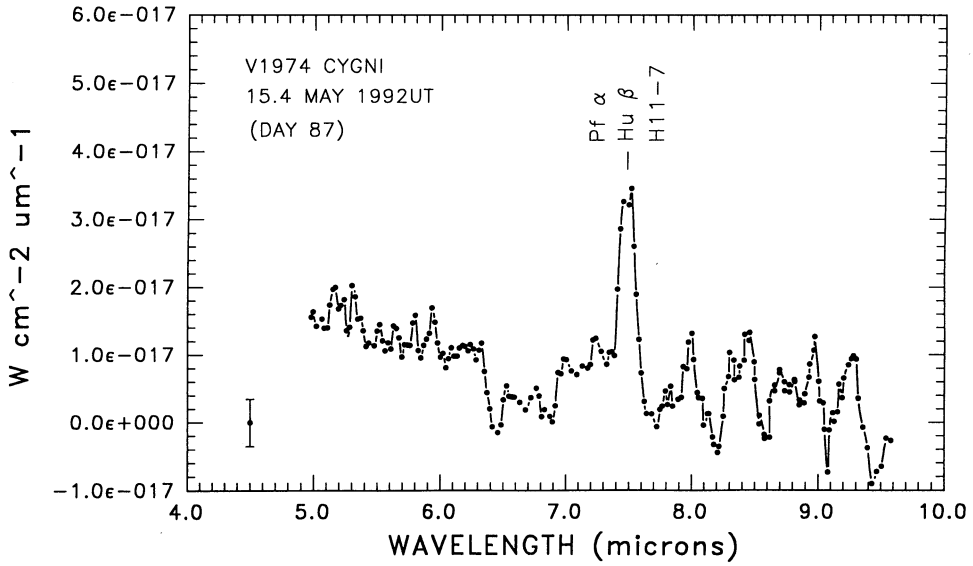


FIG. 2.—The 5–10 $\mu$m spectrum of V1974 Cyg obtained on 1992 May 15.4 UT (day 87) from the KAO. The spectrum is still dominated by hydrogen recombination lines. A representative mean 1 $\sigma$ error bar is given in the lower left of the panel.

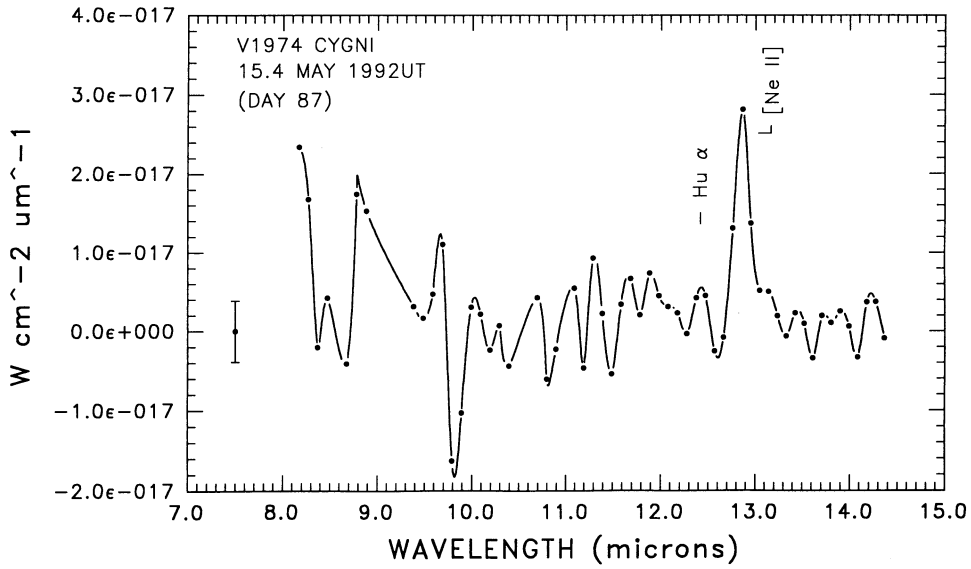


FIG. 3.—The low-resolution 7–14 $\mu$m spectrum of V1974 Cyg obtained on 1992 May 15.4 UT (day 87) from the KAO. Emission from [Ne II] is clearly evident. A representative mean 1 $\sigma$ bar is given in the lower left of the panel.

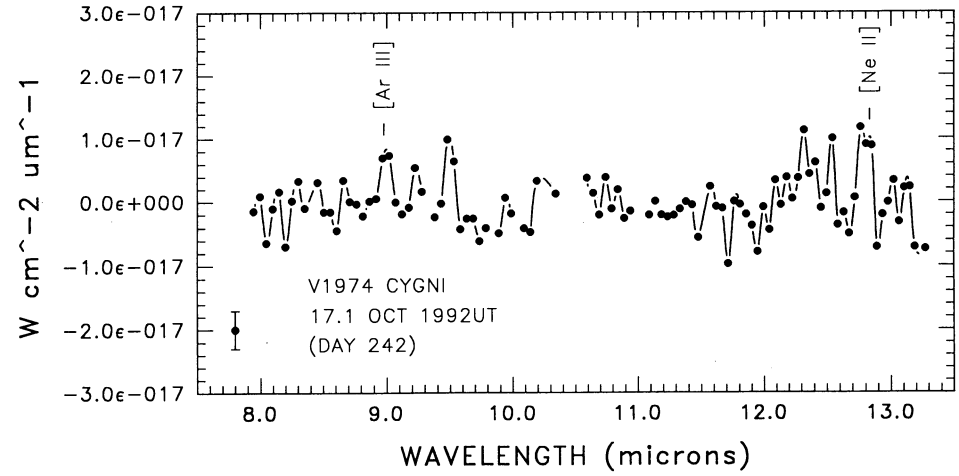


FIG. 4.—The 8–13 $\mu$m spectrum of V1974 Cyg obtained on 1992 October 17.1 UT (day 242) from the NASA 1.52 m infrared telescope facility on Mount Lemmon, AZ. Emission lines of [Ar III] and [Ne II] are evident in the spectrum. A representative mean 1 $\sigma$ error bar is given in the lower left of the panel. The gap in the spectrum near 10.5 $\mu$m is due to a noise spike.

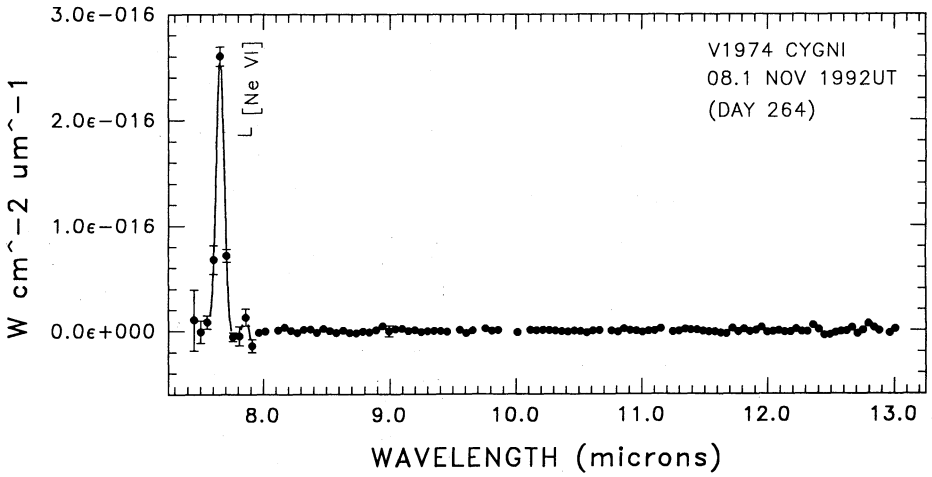


FIG. 5.—The 7–13 $\mu$m spectrum of V1974 Cyg obtained on 1992 November 8.1 UT (day 264) from the NASA 1.52 m infrared telescope facility on Mount Lemmon, AZ. A strong [Ne VI] emission line dominates the emergent spectra. A representative mean 1 $\sigma$ error bar is given in the lower left of the panel.

have identified the principal lines, which include hydrogen lines, forbidden lines of [Ar III] and [Ne II], and an infrared coronal line of [Ne VI]. Integrated line fluxes for lines that are clearly identified ($\geq$two channels wide) in our spectra are presented in Table 1.

In May ($\approx$day 80), the dominant emission lines in the mid-infrared spectra were a blend of three hydrogen lines (Pf$\alpha$, Hu$\beta$, H11–7) near 7.5 $\mu$m and [Ne II] at 12.8 $\mu$m. During the next 170 days, the hydrogen emission virtually disappeared, the [Ne II] 12.8 $\mu$m line weakened considerably, and a pronounced line due to [Ne VI] at 7.60 $\mu$m had appeared. Our spectra suggest that the temporal development of the mid-infrared hydrogen and the neon emission is similar to the evolution of the near-infrared hydrogen, aluminum, and magnesium coronal lines observed in V1974 Cyg by Woodward et al. (1993, 1994). We find this decline in the hydrogen recombination lines preceding the onset of the coronal line emission phase in V1974 Cyg is characteristic of all infrared coronal line novae observed to date.

This temporal evolution is produced by changing ionization conditions in the ejecta rather than the available excitation for the coronal forbidden lines. Infrared coronal lines are low ($\approx 10^{3-5}$ K) excitation temperature, high critical density ($\approx 10^{6-9}$ cm$^{-3}$) forbidden-line transitions of heavy ions with ionization potential $\chi \geq 100$ eV (Greenhouse et al. 1990, 1993). As a consequence, the spectral evolution that we observe among the hydrogen recombination lines and infrared coronal lines is not governed by the energy spectrum of electrons which excite the coronal lines. Rather, this evolution traces a rapid increase of the ionization state of the ejecta. This increase in the overall level of ionization can be due to either an increase in the kinetic temperature of the ejecta or hardening of the ionizing radiation field of the nova remnant. In the former case, the hydrogen recombination lines are suppressed as a result of the temperature dependence of their recombination coefficients $T_e(K)^{-0.75}$ (Spitzer 1978).

### 3.1. *Ionization Temperature and Elemental Abundances*

Infrared coronal lines provide a primary means to determine elemental abundances in novae ejecta. The specific intensity $I_{ij}$ due to a transition $j \rightarrow i$ in ion $X^{+p}$ is

$$I_{ij} = A_{ji} \frac{hc}{\lambda_{ij}} \frac{n(X_j^{+p})}{n(X_{tot}^{+p})} \frac{n(X_{tot})}{n(H)} \frac{ln_e}{4\pi} \text{ ergs s}^{-1} \text{ cm}^{-2} \text{ sr}^{-1}, \quad (1)$$

where $hc/\lambda_{ij}$ is the photon energy, $A_{ji}$ is the spontaneous transition probability, $n(X_j^{+p})/n(X_{tot}^{+p})$ is the relative population of the level $j$ in the ion $X^{+p}$, $n(X^{+p})/n(X_{tot})$ is the relative abundance of the ionization state $p$ of element X, $n(X)_{tot}/n(H)$ is the gas phase chemical abundance of X, $n_e$ is the electron density, and $l$ is the column length through the emitting region. Values for $\lambda$, $A_{ji}$, and level populations $n(X_j^{+p})/n(X_{tot}^{+p})$ for the transitions discussed here are given in Greenhouse et al. (1993).

The electron temperature in the coronal line emitting region of V1974 Cyg can be determined from coronal lines of adjacent ionization states such as the [Si VI] 1.959 $\mu$m/[Si VII] 2.474 $\mu$m line ratio along with level populations from Greenhouse et al.

TABLE 1

OBSERVED LINE FLUXES OF V1974 CYGNI

| ION | TRANSITION ($i \leftarrow j$) | OBSERVED WAVELENGTH ($\mu$m) | FLUX[a] 1992 May 15 (Day 87) | 1992 Oct 17 (Day 242) | 1992 Nov 8 (Day 264) |
|---|---|---|---|---|---|
| [Ne VI] ..... | $^2P_{1/2}$–$^2P_{3/2}$ | 7.65 | ... | ... | 217.87 ± 9.23 |
| [Ar III] ..... | $^3P_2$–$^3P_1$ | 8.99 | ... | 7.66 ± 2.76 | ... |
| Hu $\alpha$ ..... | 6–7 | 12.37 | ... | 9.80 ± 3.62 | 2.84 ± 1.27 |
| [Ne II] ..... | $^2P_{1/2}$–$^2P_{3/2}$ | 12.81 | 58.98 ± 15.68 | 12.86 ± 4.99 | 4.51 ± 1.27 |

[a] Fitted line flux ($\times 10^{-19}$ W cm$^{-2}$).

(1993) and equation (1). Thus,

$$\frac{I\lambda 1.959}{I\lambda 2.474} = 2.033 \frac{n(\mathrm{Si}^{+5}_{^2P_{1/2}})}{n(\mathrm{Si}^{+6}_{^3P_1})} \frac{n(\mathrm{Si}^{+5}_{\mathrm{tot}})}{n(\mathrm{Si}^{+6}_{\mathrm{tot}})}. \quad (2)$$

The equilibrium value of the last term on the right is independent of density and provides a measure of the ionization temperature (Fig. 6*a*). The middle term on the right is density dependent at densities approaching the critical densities of the transitions (Figs. 6*b* and 6*c*). Using [Si VI] and [Si VII] line intensities reported by Dinerstein et al. (1992) for days 233, 258, and 295, we estimate that $I\lambda 1.959/I\lambda 2.474 \approx 1.3$ on day 264 of our KAO [Ne VI] observation. Hayward et al. (1992) estimate an electron density in the ejecta of $\approx 4 \times 10^7$ cm$^{-3}$ on day 54. If we assume that no additional mass injection into the ejecta has occurred and that this material expanded at constant velocity (Pendelton et al. 1992; Greenhouse et al. 1992) in a shell of constant thickness from day 54 to day 264, the temporal evolution of $n_e$ is $\approx t_{\mathrm{days}}^{-2}$ (Ennis et al. 1977). Thus, we estimate on day 264 $n_e \approx 1.7 \times 10^6$ cm$^{-3}$.

The neon abundance in the coronal zone of the ejecta can be estimated using equation (1) and the [Ne VI] 7.642 $\mu$m/[Si VI] 1.959 $\mu$m intensity ratio. Therefore,

$$\frac{I\lambda 7.642}{I\lambda 1.959} = 0.002 \frac{n(\mathrm{Ne}^{+5}_{^2P_{3/2}})}{n(\mathrm{Si}^{+5}_{^2P_{1/2}})} \frac{n(\mathrm{Ne}^{+5}_{\mathrm{tot}})}{n(\mathrm{Si}^{+5}_{\mathrm{tot}})} \frac{n(\mathrm{Ne})}{n(\mathrm{Si})}. \quad (3)$$

Figure 7 shows the ionization temperature and density dependence of this line ratio for a solar photospheric abundance pattern of $[n(\mathrm{Ne})/n(\mathrm{Si})]_\odot = 0.347$ (Grevesse & Anders 1989). The measured line ratio determined using our day 264 KAO data on [Ne VI] and ground-based data on [Si VI] reported by Dinerstein et al. (1992) also is plotted in the figure (*filled circle*). We find a [Ne VI] 7.642 $\mu$m/[Si VI] 1.959 $\mu$m intensity ratio of $20.3 \pm 1.8$, in excess of the line ratio expected for a solar Ne/Si abundance pattern at $n_e \approx 10^6$ cm$^{-3}$, $I\lambda 7.642/I\lambda 1.959 \approx 2.543$. We note that since $\mathrm{Ne}^{+5}$ and $\mathrm{Si}^{+5}$ have approximately the same characteristic ionization temperature of $\approx 4 \times 10^5$ K (Greenhouse et al. 1993), the abundance derived below is relatively insensitive to the assumed temperature and density of the ejecta (Fig. 7).

Although the large [Ne VI]/[Si VI] line ratio we observe could, in principle, result from gas phase depletion of silicon by dust formation, we find no evidence for the 10 $\mu$m and 20 $\mu$m emission features from silicate grains at this epoch. In addition, novae that exhibit pronounced infrared coronal lines often exhibit optical coronal lines of iron (e.g., Ferland & Shields 1978; Wallerstein & Garnavich 1986), suggesting that refractory elements are not appreciably depleted during the coronal line emission phase of novae. We conclude that the ratio $(\mathrm{Ne/Si})_{\mathrm{V1974\,Cyg}}/(\mathrm{Ne/Si})_\odot \approx 9.8$ is due primarily to a large ($\sim 10$) overabundance of neon in the ejecta.

### 3.2. *Sodium in V1974 Cygni*

We have used our day 242 spectra to estimate an upper limit to the Na abundance in V1974 Cyg from the upper limits to the fluxes from the [Na III] 7.319 $\mu$m and [Na IV] 9.039 $\mu$m lines.

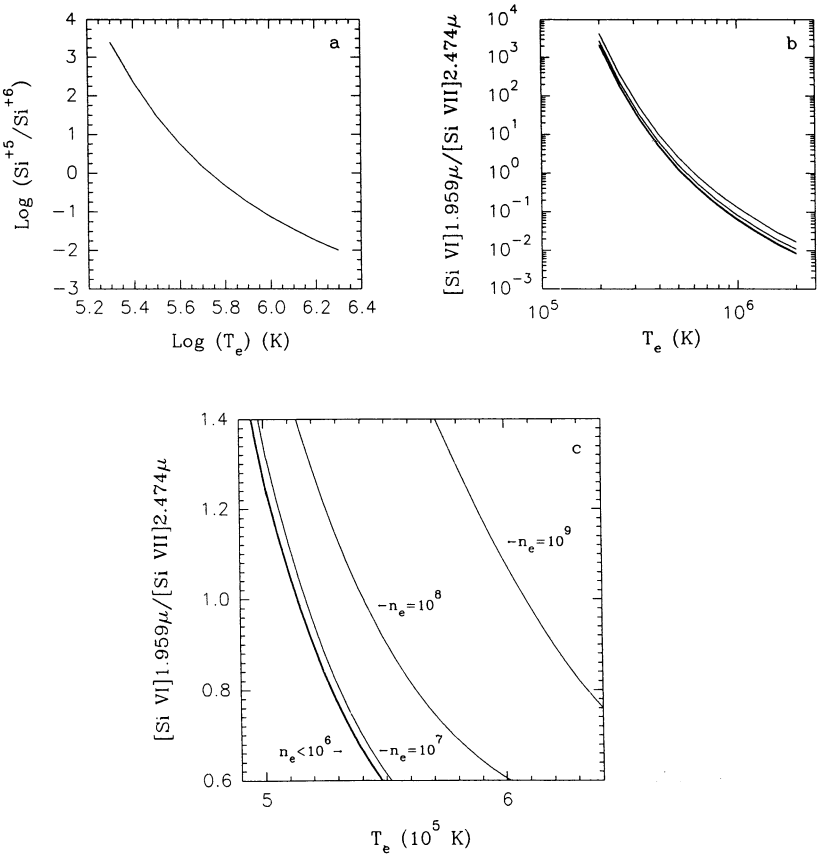


FIG. 6.—The coronal ionization equilibrium of $\mathrm{Si}^{+5}$ and $\mathrm{Si}^{+6}$ as a function of (*a*) temperature, and (*b*) and (*c*) corresponding [Si VI] 1.959 $\mu$m/[Si VII] 2.474 $\mu$m line intensity ratio at several densities. Fig. 6*a* is independent of density. Densities in Figs. 6*b* and 6*c* are shown in units of cm$^{-3}$. Further details are discussed in § 3.1.

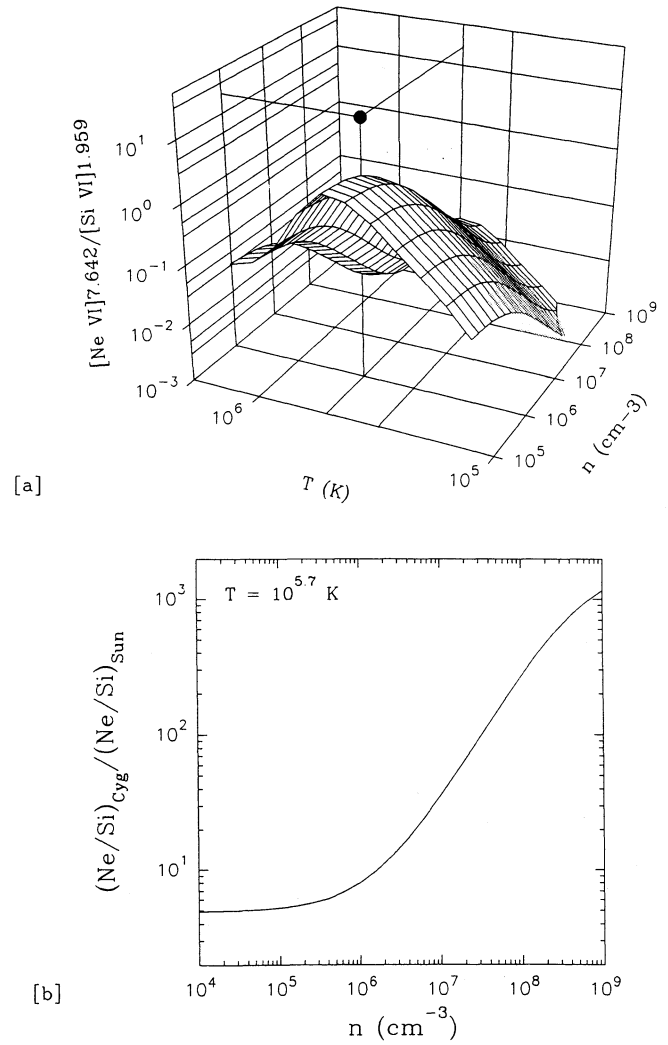


FIG. 7.—(*a*) The calculated [Ne VI] 7.642 $\mu$m/[Si VI] 1.959 $\mu$m intensity ratio of V1974 Cyg (§ 3.1, eq. [3]) is shown as a function of ionization temperature and electron density for solar photospheric abundances of Ne and Si. The day 264 measured line ratio is plotted as a solid dot. All axes are logarithmic. (*b*) The derived overabundance of Ne/Si as a function of assumed electron density. We find that at any reasonable density and temperature, a factor of $\approx 10$ overabundance of neon with respect to silicon is required to account for the observed ratio. Further details are discussed in § 3.1.

The Na abundance provides a useful test for models of TNR ONeMg in novae. Theoretical studies of TNRs in the accreted envelopes of ONeMg white dwarfs predict that substantial amounts of $^{26}$Al and $^{22}$Na can be produced in nova explosions (Nofar, Shaviv, & Starrfield 1990; Starrfield et al. 1992b). However, the relative production rate of these two species is a strong function of the mass of the white dwarf progenitor and the temperature history of the TNR. Indeed, a strong anticorrelation between $^{26}$Al and $^{22}$Na production in nova outbursts has been suggested (Starrfield et al. 1992b). It is important to try to verify these predictions since the amount of $^{22}$Na is dependent strongly on the peak temperature reached in the explosion and measuring its abundance will provide information on the evolutionary behavior of the TNR occurring far below the surface of the white dwarf.

While the abundance of aluminum can be determined from emission lines in the wavelength regions sampled by the *IUE* satellite, it is not possible to obtain the isotopic abundance, and the evolutionary studies imply that a fraction of the observed aluminum is $^{27}$Al and not $^{26}$Al. Therefore, it also is necessary to predict the total amount of aluminum in the ejecta and compare that value to the observed amount of sodium.

Since $^{22}$Na is radioactive, with a $\approx 2.6$ yr half-life, it is possible to use *Compton GRO* to determine the amount of this isotope in the ejecta (Starrfield et al. 1992b). This determination has already been tried with V1974 Cyg with apparently negative results, although a much lower exposure has been proposed (Leising et al. 1993). Earlier the sodium abundance in a novae was determined from a nebular emission line at 2069 Å (Williams et al. 1985). However, it was recently shown that this line is produced by Ne III (Shore et al. 1994). Thus, ultraviolet lines cannot be used to infer the sodium abundance. Infrared coronal lines of sodium can provide an accurate determination of the sodium abundance in ONeMg novae. We emphasize that it is necessary to measure both the total abundance of sodium with the KAO by observing the [Na III] 7.319 $\mu$m, [Na IV] 9.039 $\mu$m, and [Na IV] 21.29 $\mu$m lines, and to combine these measurements with a determination of the isotopic abundance of $^{22}$Na from *Compton GRO* to obtain the $^{23}$Na abundance which can also be predicted from the theoretical studies.

Abundances deduced from mid-infrared spectroscopy of V1974 Cyg can provide a clear test of the hydrodynamic simulations. V1974 Cyg was classified as a "neon" nova (ONeMg progenitor) with the discovery of [Ne II] emission on day 54 (Hayward et al. 1992). This finding was confirmed by *IUE* spectral studies of the line profiles (Shore et al. 1993). Our data give an approximate upper limit of $\leq 7 \times 10^{-19}$ W cm$^{-2}$ (3 $\sigma$) to the [Na III] 7.319 $\mu$m and [Na IV] 9.039 $\mu$m in V1974 Cyg on day 242.

In order to estimate expected infrared line intensities from transient sodium enrichment in V1974 Cyg and other ONeMg novae, we performed new detailed balance calculations of the [Na III] 7.319 $\mu$m, [Na IV] 9.039 $\mu$m, and [Na IV] 21.29 $\mu$m lines. Greenhouse et al. (1993) have previously performed these calculations for [Na VII] 4.675 $\mu$m, [Na VI] 8.61 $\mu$m, and [Na VI] 14.3 $\mu$m. Transitions of argon within the bandpass of interest are also included for completeness. Atomic constants, critical densities, and emissivities for these transitions are given in Table 2. Column designations in the Table are as follows: (1) ion; (2) transition; (3) calculated or measured wavelength denoted as c or m respectively, where the standard error of the last digit follows in parentheses ( ) and calculated wavelengths are given in vacuum; (4) spontaneous transition rate $A_{ji}$; (5) ionization potential; (6) ion characteristic temperature $T_{max} \equiv$ the equilibrium temperature of maximum ion concentration $n(X^{+i})/n(X_{tot})$ in a collisionally ionized plasma; (7) transition excitation temperature $E_j/k$, where $E_j$ is the energy of the upper level of the transition and $k$ is the Boltzmann's constant; (8) transition critical density; and (9) intrinsic photon rate $\log (A_{ji} n_j/n_e)|_{<n_{crit}}$ photons s$^{-1}$ ion$^{-1}$, where $n_j$ is the relative population of the level $j$.

The data in columns (3)–(7) of Table 2 are archival. Wavelengths and transition probabilities given in columns (3) and (4) were extracted from a larger compilation of forbidden lines produced by Kaufman & Sugar (1986). Ionization potentials were taken from Allen (1981). Characteristic temperatures were taken from Landini & Fossi (1972) and Shull & Van Steenberg (1982). References for energy levels and measured wavelengths are given in Kaufman & Sugar (1986). Measured wavelengths have been used in Table 2 whenever possible. Energy level

TABLE 2

INFRARED FORBIDDEN LINES WITHIN THE GROUND $2s^2 2p^k$, $3s^2 3p^k$ CONFIGURATIONS OF ARGON AND SODIUM LOW ($\chi < 100$ eV) IONIZATION STATES[a]

| Species (1) | Transition ($i \leftarrow j$) (2) | $\lambda$ ($\mu$m) (3) | $A_{ji}$ ($s^{-1}$) (4) | $\chi$ (eV) (5) | log $T_{max}$ (K) (6) | log $(E_j/k)$ (K) (7) | $n_{crit}$ ($cm^{-3}$) (8) | $-\log (A_{ji} n_j/n_e)|_{<n_{crit}}$ (photon $s^{-1}$ $ion^{-1}$) (9) |
|---|---|---|---|---|---|---|---|---|
| Ar III ..... | $^3P_2$–$^3P_1$ | m, 8.9910(1) | $3.06e-2$ | 40.74 | 4.7 | 3.2 | 5.5 | 7.7 |
| Ar III ..... | $^3P_1$–$^3P_0$ | c, 21.842(6) | $5.31e-3$ | 40.74 | 4.7 | 3.4 | 4.8 | 8.1 |
| Na III ..... | $^3P_3$–$^3P_{1/2}$ | c, 7.319(5) | $4.59e-2$ | 71.64 | 4.9 | 3.3 | 6.7 | 8.5 |
| Na IV ..... | $^3P_2$–$^3P_1$ | c, 9.039(12) | $3.04e-2$ | 98.91 | 5.3 | 3.2 | 6.2 | 8.4 |
| Na IV ..... | $^3P_1$–$^3P_0$ | c, 21.29(6) | $5.58e-3$ | 98.91 | 5.3 | 3.4 | 5.6 | 8.9 |

[a] Higher ionization states $\chi \geq 100$ eV are treated in Greenhouse et al. 1993.

diagrams for the relevant configuration of each ion listed in Table 2 are given in Greenhouse et al. (1993). Readers should cite original references when referring to archival data presented in Table 2.

The relative intensities of the transitions listed in Table 2 can be assessed using column (9) where we have listed the intrinsic photon rate per ion, $\log (A_{ji} n_j/n_e)|_{<n_{crit}}$, derived from the results of our detailed balance calculations. Level populations were obtained by solving the set of coupled rate equations

$$n_j\left[\sum_{i<j} A_{ji} + n_e\left(\sum_{i<j} C_{ji} + \sum_{i>j} C_{ji}\right)\right] = n_e\left(\sum_{i<j} n_i C_{ij} + \sum_{i>j} n_i C_{ij}\right) + \sum_{i>j} n_i A_{ij}\,, \quad (4)$$

where $n_i \equiv n(X_i^{+p})/n(X_{tot}^{+p})$ and $n_j \equiv n(X_j^{+p})/n(X_{tot}^{+p})$ are the relative populations of the levels $i$ and $j$ in the ion $X^{+p}$. These populations were calculated using the Hebrew University Lawrence Livermore Atomic Code (HULLAC) and are shown in Figures 8 and 9, where the quantity $\log (n_j/n_e)$ is plotted as a function of electron density $n_e$. This quantity is constant for $n_e \ll n_{crit}$ and extrapolates linearly to $n_e \gg n_{crit}$. The critical density $n_{crit}$ for collisional deexcitation of the level occurs at the knee of the curve. Further details and additional results for infrared emission from higher ionization states of sodium and other abundant elements can be found in Greenhouse et al. (1993).

Recent models (Starrfield et al. 1992a, b) suggest that a Na/Si abundance ratio of $\simeq 0.132$ can occur in the ejecta of classical novae that occur on 1.35 $M_\odot$ ONeMg white dwarfs. Such ONeMg novae as V1974 Cyg, Nova Cyg 1986, V827 Her, QU Vul, and V1500 Cyg evolve through an infrared coronal emission line phase during which pronounced [Si VI] 1.959 $\mu$m and [Si VII] 2.474 $\mu$m emission is observed (Dinerstein et al. 1992; Greenhouse et al. 1990; Benjamin & Dinerstein 1990; Gehrz 1988, 1990). To facilitate sodium abundance determinations for ONeMg novae during this bright infrared emission line phase, we present model [Na VII] 4.675 $\mu$m/[Si VII] 2.474 $\mu$m, [Na VI] 8.61 $\mu$m/[Si VII] 1.959 $\mu$m, and [Na VI] 14.3 $\mu$m/[Si VI] 1.959 $\mu$m intensity ratios determined using equation (1) and data from Greenhouse et al. (1993). These results are shown in Figure 10 for two ionization temperatures ($T = 10^{5.4}$ K and $10^{5.8}$ K) that encompass typical coronal zone ionization temperatures for these novae (§ 3.1; Greenhouse et al. 1990). We use the maximum Na/Si abundance ($\approx 0.132$) predicted by Starrfield et al. (1992a) and the day 264 [Si VI] and [Si VII] fluxes from Dinerstein et al. (1992) to predict the infrared sodium line emission strength in V1974 Cyg. For shell densities

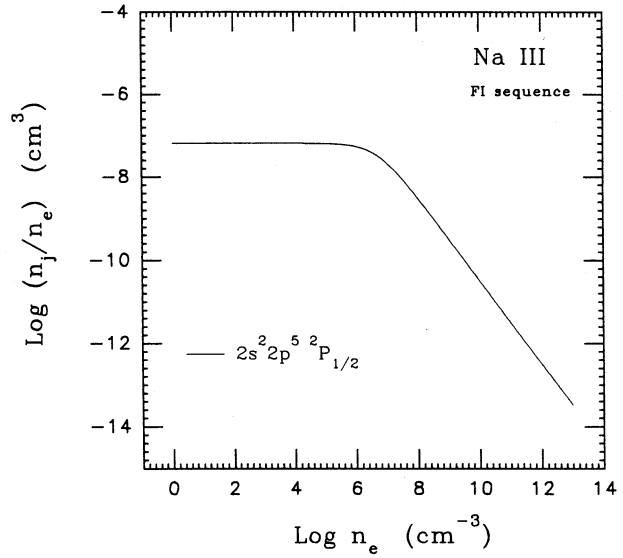


FIG. 8.—Level populations $n_j \equiv n(Na_j^{+2})/n(Na_{tot}^{+2})$ as a function of electron density $n_e$. The critical density for collisional deexcitation of the indicated level occurs at the knee of the curve (see Table 2).

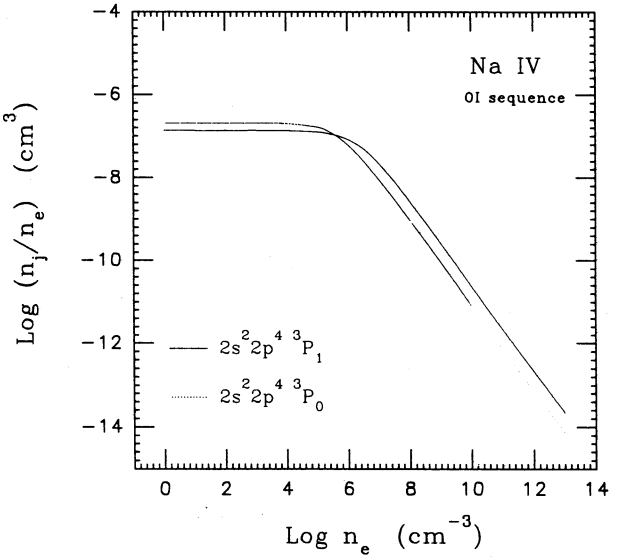


FIG. 9.—Level populations $n_j \equiv n(Na_j^{+3})/n(Na_{tot}^{+3})$ as a function of electron density $n_e$. The critical density for collisional deexcitation of the indicated level occurs at the knee of the curve (see Table 2).

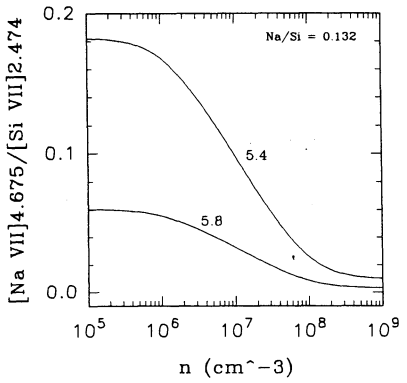


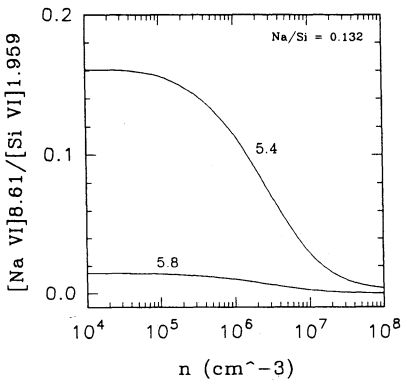


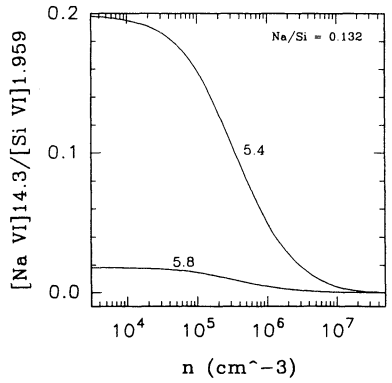


FIG. 10.—Intensity ratios among sodium and silicon infrared coronal lines are shown as a function of density at ionization temperatures of $T = 10^{5.4}$ K and $10^{5.8}$ K. The assumed Na/Si abundance ratio of 0.132 corresponds to a model prediction of Starrfield et al. (1992a) for a classical nova outburst on a 1.35 $M_\odot$ ONeMg white dwarf. Further details are discussed in § 3.2.

in the range of $10^6 < n_e$ (cm$^{-3}$) $< 10^7$, V1974 Cyg would have exhibited [Na VI] and [Na VII] intensities ($10^{-13}$ ergs s$^{-1}$ cm$^{-2}$) in the range of $3.7 > I\lambda 8.61\ \mu m > 0.3$, $15.1 > I\lambda 14.3\ \mu m > 8.8$, and $2.8 > I\lambda 4.675\ \mu m > 0.2$ if this Na/Si ratio were achieved.

We find that the day 264 [Na VI] 8.61 $\mu$m intensity predicted above is roughly an order of magnitude below the 3 $\sigma$ detection limit of the HIFOGS observations. The [Na VI] 14.2 $\mu$m line cannot be observed from the KAO as a result of telluric $CO_2$ absorption. However, we note that the [Na VII] 4.675 $\mu$m emission could be detected using the facility cryogenic echelle spectrometer (CSHELL) of the NASA Infrared Telescope Facility—IRTF (Greene, Denault, & Tokunaga 1992). Finally, we note that all of the above predicted intensities are large relative to the limiting sensitivity of the *Infrared Space Observatory* (*ISO*) Short Wavelength Spectrometer (Encrenaz & Kessler 1992).

## 4. CONCLUSIONS

Our analysis of the 4—14 $\mu$m infrared spectra of V1974 Cyg leads to several conclusions:

1. The [Ne VI] 7.65 $\mu$m emission line was observed for the second time in an ONeMg nova, and for the first time with sufficient spectral resolution and sensitivity to support an abundance determination. The ratio of Ne/Si in V1974 Cyg was $\approx 10$ times the solar photospheric ratio. Since models and observations show it is unlikely that Si is significantly depleted with respect to hydrogen in ONeMg novae TNRs, we can infer that Ne/H in V1974 Cyg exceeded that of the solar photosphere by $\approx 10$.

2. The temporal evolution of V1974 Cyg appears similar to that of the prototype neon nova QU Vul in terms of the sequence of appearance of the various forbidden emission lines.

3. The abundance of sodium in V1974 Cyg is not well determined by the present observations. We conclude from model calculations that forbidden sodium emission lines could be detected in novae of similar brightness using the NASA IRTF CSHELL spectrometer and by *ISO*.

We are pleased to acknowledge the cooperation and support of the staff of the KAO and the NASA/Steward 1.52 m telescope at Mt. Lemmon, Arizona. R. D. G., C. E. W., and S. G. S. were supported by NASA contract NAG 2-755 for observations on the KAO. M. A. G. was supported in part by NASA grant NAG 1-711 and the Smithsonian Institution Scholarly Studies Program. We thank H. Dinerstein and R. Benjamin for their silicon line intensity data prior to publication and T. J. Jones for a critical reading of the manuscript.

## REFERENCES

Allen, C. W. 1981, Astrophysical Quantities (3d ed.; London: Athlone)
Benjamin, R., & Dinerstein, H. L. 1990, AJ, 100, 1588
Cohen, M., Witteborn, F. C., Carbon, D. F., Augason, G., Wooden, D., Bregman, J., & Goodvitch, D. 1992, AJ, 104, 2045
Dinerstein, H. L., Benjamin, R. A., Gaffney, N. I., Lester, D. F., & Ramseyer, T. F. 1992, BAAS, 24, 1189
Dopita, M., et al. 1993, ApJ, in press
Encrenaz, T., & Kessler, M. 1992, in Infrared Astronomy with ISO (New York: Nova Science)
Ennis, D., Becklin, E. E., Beckwith, S., Elias, J., Gatley, I., Matthews, K., Neugebauer, G., & Willner, S. P. 1977, ApJ, 214, 478
Ferland, G. J., & Shields, G. A. 1978, ApJ, 226, 172

Gehrz, R. D. 1988, ARA&A, 26, 377
———. 1990, in Physics of Classical Novae, ed. A. Cassatella & R. Viotti (Berlin: Springer-Verlag), 138
Gehrz, R. D., Grasdalen, G. L., & Hackwell, J. A. 1985, ApJ, 298, L47. Erratum 1986, ApJ, 306, L49
Gehrz, R. D., Lawrence, G. F., & Jones, T. J. 1992, IAU Circ., No. 5463
Gehrz, R. D., Truran, J. W., & Williams, R. E. 1991, in Protostars and Planets III, ed. E. Levy & J. Lunine (Tucson: Univ. of Arizona Press), in press
Greene, T., Denault, A., & Tokunaga, A. 1992, Cryogenic Echelle Spectrograph User's Manual (Honolulu: NASA Infrared Telescope Facility)
Greenhouse, M. A., Feldman, U., Smith, H. A., Klapisch, M., Bhatia, A. K., & Bar-Shalom, A. 1993, ApJS, 88, 23
Greenhouse, M. A., Grasdalen, G. L., Hayward, T. L., Gehrz, R. D., & Jones, T. J. 1988, AJ, 95, 172
Greenhouse, M. A., Grasdalen, G. L., Woodward, C. E., Benson, J., Gehrz, R. D., Rosenthal, E., & Skrutskie, M. F. 1990, ApJ, 352, 307
Greenhouse, M. A., Woodward, C. E., Fischer, J., & Smith, H. A. 1992, IAU Circ., No. 5674
Grevesse, N., & Anders, E. 1989, in Cosmic Abundances of Matter, ed. C. J. Waddington (New York: AIP), 1
Hayward, T., Gehrz, R. D., Miles J. W., & Houck, J. R. 1992, ApJ, 401, L101
Kaufman, V., & Sugar, J. 1986, J. Phys. Chem. Ref. Data, 15 (1), 321
Landini, M., & Fossi, B. C. 1972, A&A, 7, 291
Leising, M., et al. 1993, in Proc. 2nd Compton Conference (AIP Conf. 280), ed. M. Freedlander, N. Gehrels & D. J. McComb (New York: AIP), in press
Nofar, I., Shaviv, G., & Starrfield, S. 1990, ApJ, 369, 440
Pendelton, Y., Gehrz, R. D., Kaminski, C., Jennerjohn, N., Sandford, S., & Allamandola, L. 1992, IAU Circ., No. 5544
Saizar, P., et al. 1992, ApJ, 398, 651
Shore, S., et al. 1994, in preparation
Shull, M., & Van Steenberg, M. 1982, ApJS, 48, 95
Spitzer, L. 1978, Physical Processes in the Interstellar Medium (New York: J. Wiley & Sons)
Starrfield, S., Shore, S. N., Sparks, W. M., Sonneborn, G., Truran, J. W., & Politano, M. 1992a, ApJ, 391, L71
Starrfield, S., Sparks, W. M., & Truran, J. W. 1986, ApJ, 303, L5
Starrfield, S., Truran, J. W., Politano, M., Sparks, W. M., Nofar, I., & Shaviv, G. 1992b, in Proc. Workshop to Honor W. A. Fowler on his 80th Birthday, ed. S. Woosley, in press
Walker, R. G., & Cohen, M. 1992, An Atlas of Selected Calibrated Stellar Spectra, Final Report Contract NAG 2-13327, NASA/Ames Research Center
Wallerstein, G., & Garnavich, P. 1986, PASP, 96, 875
Williams, R. E., Ney, E. P., Sparks, W. M., Starrfield, S., & Truran, J. W. 1985, MNRAS, 212, 753
Witteborn, F. C., Bregman, J. D., Rank, D. M., & Cohen, M. 1991, in Proc. of the 1991 North American Workshop on Infrared Spectroscopy, ed. R. E. Stencel (Boulder: Univ. Colorado), 29
Woodward, C. E., & Gehrz, R. D. 1992, IAU Circ., No. 5617
Woodward, C. E., et al. 1993, BAAS, 24, 1189
Woodward, C. E., Greenhouse, M. A., Gehrz, R. D., Pendelton, Y., Allamandola, L., Sandford, S., Joyce, R. R., & Van Buren, D. 1994, in preparation